β-Lactone Synthesis from Epoxide and CO: Reaction Mechanism Revisited

András Stirling,*,† Marcella Iannuzzi,‡ Michele Parrinello,† Ferenc Molnar,§ Volker Bernhart,§ and Gerrit A. Luinstra§

Department of Chemistry and Applied Biosciences, ETH Zurich, Switzerland, Institute of Physical Chemistry, University of Zurich, Zurich, Switzerland, and BASF AG, Ludwigshafen, Germany

Received March 22, 2005

The formation of β-lactone from epoxide and CO catalyzed by $CoCO_4^-$ has been studied using a novel ab initio molecular dynamics approach. Employing the so-called metadynamics methodology, we show that it is possible to unravel the reaction mechanism of the catalyzed lactone formation in a fairly unbiased way. We were able to reproduce all the elementary steps within relatively short simulation time: the epoxide opening, the CO insertion, the CO addition to the Co site, the lactone ring formation, and the product dissociation, as obtained in previous static calculations. In addition, the simulations revealed that the lowest energy path goes through a stable intermediate featuring a metalla-oxo-furanyl ring. The simulations also indicated a new, higher energy path, in which the lactone ring formation precedes the CO uptake of the Co center. We show that this route becomes competitive when the Lewis acid attached to the lactone oxygen is softer.

Introduction

Efficient control of chemical reactions is in many cases only achievable by catalysis. It is therefore of the utmost importance to understand the functionality of the catalytic species involved in the chemical reaction. Leaving aside for the moment the large fields of heterogeneous and enzymatic catalysis, homogeneous catalysis is currently dominated by organometallic chemistry[1] with relatively small catalytic species on the order of 10^2 atoms. The concept of "single-site catalysis", involving at its core a single well-defined catalytic molecular entity, has shown its value in many cases;[2] however for more difficult cases "multisite catalysis" is the key to achieving efficient processes.[3]

The formation of β-lactones through the cobalt-catalyzed carbonylation of epoxides has been observed in a number of cases.[4] Recently, we have proposed a reaction mechanism[5] based on quantum chemical calculations in the spirit of transition state theory.[6] Formulation of the reaction mechanism in ref 5 was guided mainly by chemical intuition. As usual in this line of work, starting structures for transition states are initially guessed and then optimized to find the nearest saddle point. Starting from the saddle point, the actual transition state, reactant, and product valleys are visited on the energy hypersurface. The reaction mechanism is then put together by connecting reactants and products through a sequence of intermediates, which are separated by transition states. In general, this is a sound approach if at least part of the reaction pathway is known or can safely be derived from well-known chemical reaction mechanisms. However, there is always the danger of overlooking reaction pathways that are not close to the well-known pathways of (organometallic) chemistry. Therefore we decided to reinvestigate the proposed reaction mechanism of carbonylation of epoxides (cf. Figure 1) by a cobalt catalyst[5] with the help of ab initio molecular dynamics, using a methodology that allows the observation of "rare events" such as chemical reactions at moderate temperature. In this

* To whom correspondence should be addressed. E-mail: stirling@phys.chem.ethz.ch.
† ETH Zurich.
‡ University of Zurich.
§ BASF AG.

(1) (a) Cornils, B.; Herrmann W. A. *Applied Homogeneous Catalysis with Organometallic Compounds*, 2nd ed.; Wiley-VCH: Weinheim, 1999. (b) Kirchner, K.; Weissensteiner W. *Organometallic Chemistry and Catalysis*; Springer: Wien, 2001.

(2) (a) Ivin, K. J.; Mol J. C. *Olefin Metathesis and Metathesis Polymerization*: Academic Press: San Diego, CA, 1997. (b) Furstner, A.; Ackermann L.; Gabor B.; Goddard R.; Lehmann C. W.; Mynott R.; Stelzer F.; Thiel O. R. *Chem. Eur. J.* **2001**, *7*, 3236−325. (c) Hoveyda, A. H.; Schrock R. R. *Chem. Eur. J.* **2001**, *7*, 945−950. (d) Schrock, R. R. *J. Chem. Soc., Dalton Trans.* **2001**, 2541−2550. (e) Hlatky, G. G. *Coord. Chem. Rev.* **2000**, *199*, 235−329. (f) Grimmer, N. E.; Conville N. J. *S. Afr. J. Chem.* **2001**, *54*, 1−112. (g) Imanishi, Y.; Naga N. *Prog. Polym. Sci.* **2001**, *26*, 1147−1198. (h) Ittel, S. D.; Johnson L. K.; Brookhart M. *Chem Rev.* **2000**, *100*, 1169−1204. (i) Sommazzi, A.; Garbassi F. *Prog. Polym. Sci.* **1997**, *22*, 1547−1605. (j) MacQuillin, F. J. *Homogeneous Hydrogenation in Organic Chemistry*; Kluwer: Dordrecht, 1976. (k) *Rhodium Catalyzed Hydroformylation*; van Leeuwen P. W. N. M., Claver C., Eds.; Kluwer: Dordrecht, 2000. (l) Trzeciak, A. M.; Ziolkowski J. J. *Coord. Chem. Rev.* **1999**, *192*, 883−900. (m) Palucki, M.; Finney N. S.; Pospisil P. J.; Guler M. L.; Ishida T.; Jacobsen E. N. *J. Am. Chem. Soc.* **1998**, *120*, 948−954.

(3) (a) Shilov, A. E.; Shul'pin G. B. *Activation and Catalytic Reactions of Saturated Hydrocarbons in the Presence of Metal Complexes*; Kluwer Academic Publishers: Dordrecht, 2000. (b) Evans, H. J.; Bottomley P. J.; Newton W. E. *Nitrogen Fixation Research Progress*; Proceedings of the 6th International Symposium on Nitrogen Fixation, Corvallis/OR, August 4−10, 1985; Dordrecht: Nijhoff, 1985.

(4) (a) Lee, J. T.; Thomas P. J.; Alper H. *J. Org. Chem.* **2001**, *66*, 5424−26. (b) Getzler, Y. D. Y. L.; Mahadevan E. B.; Lobkosky V.; Coates G. W. *J. Am. Chem. Soc.* **2002**, *124* (7), 1174−1175, following an older patent by Drent at Shell Chemical Company: (Shell) EP 577,206. (c) Allmendinger, M.; Eberhardt R.; Luinstra G. A.; Rieger B. *J. Am. Chem. Soc.* **2002**, *125*, 5646−5647.

(5) Molnar, F.; Luinstra G. A.; Allmendinger M.; Rieger B. *Chem. Eur. J.* **2003**, *9*, 1273−1280.

(6) Truhlar, D. G.; Garrett B. C.; Klippenstein S. J. *J. Phys. Chem.* **1996**, *100*, 12771−12800.

10.1021/om0502234 CCC: $30.25
Publication on Web 04/14/2005

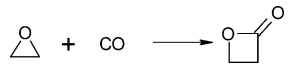

Figure 1. Carbonylation of epoxide (ethylenoxide) resulting in β-lactone formation.

approach,[7] we use a fairly unbiased technique to determine the most likely elementary steps and their sequence, and at the same time we include the dynamic aspects of the finite reaction temperature. While the method is also capable of providing accurate free energy information, in this study we exploit its capacity to generate reaction paths and stationary points (transition and intermediate states), which we refine in subsequent static quantum chemical calculations.

Models and Methods

In the ab initio molecular dynamics simulation we used a periodic version of one of the models in ref 5. In our cubic cell with a size of 15 Å × 15 Å × 15 Å the catalytically active species is a $Co(CO)_4^-$ anion. Ethylene oxide was chosen as the model epoxide, while BF_3 was used as the Lewis acid. Five CO molecules were added, according to the experimental partial CO pressure during the reaction.

To explore the reactive free energy surface, we performed Car−Parrinello molecular dynamics simulations.[8] For sampling the reactive, but necessarily rare configurations, we applied a recently developed technique, the so-called metadynamics approach.[7] In a metadynamics simulation we select a set of collective variables s_α. These variables are associated with some selected collective motions of the system, which describe the desired reaction path (e.g., stretching, bending, torsion, or other, more general coordinates). The complete system of the ionic, electronic, and collective variables is driven by the extended Lagrangian:

$$L = L_{CP} + \frac{1}{2}\sum_\alpha M_\alpha \dot{s}_\alpha^{\,2} - \frac{1}{2}\sum_\alpha k_\alpha (s_\alpha(\mathbf{R}) - s_\alpha)^2 - V(t, \mathbf{s}) \quad (1)$$

where L_{CP} is the original Car−Parrinello Lagrangian:

$$L_{CP} = \mu\sum_i \int |\dot{\phi}|^2 \, d\mathbf{r} + \frac{1}{2}\sum_I M_I \dot{\mathbf{R}}_I^{\,2} - E_{KS}[\phi_i, \mathbf{R}_I] + \sum_{ij}\Lambda_{ij}\left(\int \phi_i^{*}\phi_i \, d\mathbf{r} - \delta_{ij}\right) \quad (2)$$

The other terms in eq 1 represent the kinetic and the potential energy of the collective variables and a history-dependent potential energy, respectively. The generalized masses M_α and the coupling constants k_α determine the dynamics of the collective coordinates s_α. In eq 2 μ is the fictitious electronic mass, ϕ_i are the Kohn−Sham orbitals, M_I and R_I are the masses and coordinates of the atoms, respectively, E_{KS} is the Kohn−Sham functional, and the Λ_{ij} Lagrange multipliers enforce the orthogonality of the electronic orbitals. The $V(t, \mathbf{s})$ represents the time-dependent potential, and its role is to enhance the sampling of the configurational space. In particular, it is a sum of repulsive hill-like (Gaussian) potential terms.[7] In this study we used coordination numbers (CN) as collective coordinates. We used a derivable function of the ionic coordinates to define CN-s. For example, the CN of atom I with respect to a set of atoms j takes the following form:

$$CN_I = \sum_{j=1} \frac{1 - (R_{Ij}/R)^p}{1 - (R_{Ij}/R)^q} \qquad q > p \quad (3)$$

R_{Ij} are the instantaneous distances between the central atom I and the atoms j, whereas R is a reference bonding distance characteristic for the given $I-j$ bond. A more detailed description of the methodology is given in ref 7.

The electronic structure is described within the Kohn−Sham density functional framework, using the BLYP exchange−correlation functional.[9] The ϕ_i electronic orbitals are expanded in a plane-wave basis set up to a kinetic energy cutoff of 70 Ry. Only the valence electrons were included explicitly in the calculations, and norm-conserving pseudopotentials were used to describe the interactions between the valence electrons and the ionic cores.[10] The fictitious electronic mass was 1000 au in our simulations, and the replacement of the hydrogen atoms with deuterium allowed a time step of 0.169 fs. The simulation temperature was in all cases 350 K. The simulations were performed using the CPMD program package.[11] In the metadynamics simulations the fictitious mass M_α and coupling constants k_α were selected in all cases to be 50 and 2 au, respectively (see also ref 12). We employed different hill heights (between 2.1 and 25.1 kJ/mol) and hill widths (between 0.08 and 0.2) for the $V(t, \mathbf{s})$ in the study.

Inspecting the metadynamics trajectories and the variations of the collective coordinates we easily identify the transition and intermediate states along the reaction paths. Starting from these configurations, their equilibrium structures and energies were determined by static quantum chemical calculations. The nature of all transition states was verified (only one negative eigenvalue of the Hessian). Reactants and products were identified by inducing small distortions in the TS structure along the eigenvector associated with the negative eigenvalue. Distortions with positive and negative amplitude lead to reactants and products after subsequent geometry optimization. The static calculations were performed with the quantum-chemistry packages TURBOMOLE[13a] and Gaussian98.[13b] DFT methodology was used at the B-P86/SV(P)[9,14,15] level of theory to locate all stationary points. Single-point energy calculations were carried out using the TZVP[15] basis set.

Results and Discussion

First, we feel that it is important to discuss some significant advantages of the metadynamics method with respect to the traditional static calculations. A very important feature in the metadynamics simulation is the employment of several collective coordinates or collective variables (CV-s). The selected CV-s must be able to encompass all the chemical changes that distinguish between the reactant and product states. The reaction path and the sequence of the elementary steps are then obtained in terms of these CV-s. It is important to emphasize that the CV-s operate simultaneously

(7) (a) Iannuzzi, M.; Laio A.; Parrinello M. *Phys. Rev. Lett.* **2003**, *90*, 238302. (b) Laio, A.; Parrinello M. *Proc. Natl. Acad. Sci. U.S.A.* **2002**, *99*, 12562−12566. (c) Micheletti, C.; Laio A.; Parrinello M. *Phys. Rev. Lett.* **2004**, *92*, 170601. (d) Laio, A.; Rodriguez-Fortea A.; Gervasio F. L.; Ceccarelli M.; Parrinello M., submitted to *J. Phys. Chem. A*.

(8) Car, R.; Parrinello M. *Phys. Rev. Lett.* **1985**, *55*, 2471−2474.

(9) Becke, A. *Phys. Rev. A* **1988**, *38*, 3098−3100. Lee, C.; Yang, W.; Parr, R. *Phys. Rev. B* **1988**, *37*, 785−789.

(10) Troullier, N.; Martins, J. L. *Phys. Rev. B* **1991**, *43*, 1993−2006. Hartwigsen, C.; Goedecker S.; Hutter J. *Phys. Rev. B* **1998**, *58*, 3641−3662.

(11) CPMD V3.7 Copyright IBM Corp, 1990−2001, Copyright MPI für Festkörperforschung Stuttgart, 1997−2001.

(12) The unit of k and M depends on the actual definition of the CV.

(13) (a) Ahlrichs, R.; Bär M.; Häser M.; Horn H.; Kölmel C. *Chem. Phys. Lett.* **1989**, *162*, 165−169. (b) Frisch, M. J.; et al. *Gaussian 98*, Revision A.11.1; Gaussian, Inc.: Pittsburgh, PA, 2001.

(14) Perdew, J. P. *Phys. Rev. B* **1986**, *33*, 8822−8824; erratum in *Phys. Rev. B* **1986**, *34*, 7406−7406.

(15) Schäfer, A.; Horn H.; Ahlrichs R. *J. Chem. Phys.* **1992**, *97*, 2571−2577. Schäfer, A.; Huber C.; Ahlrichs R. *J. Chem. Phys.* **1994**, *100*, 5829−5835.

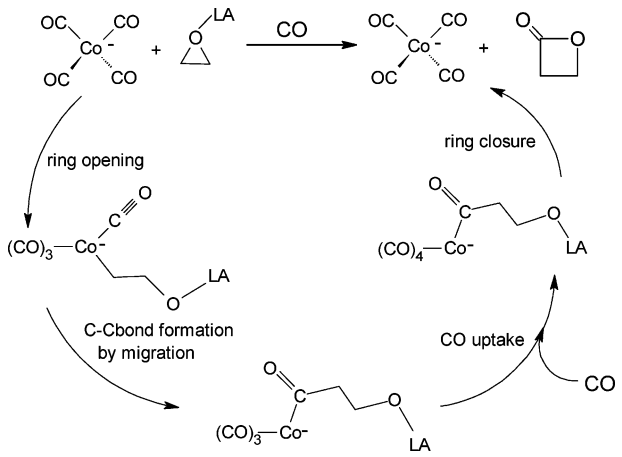

Figure 2. Original reaction scheme for the formation of lactones starting from epoxide and CO. The negative sign is always attached to the Co site, although it is delocalized in the intermediate states according to the calculations.

during the simulation, and thus the individual elementary steps can be any arbitrary combination of them. During the simulations, the height, the width, and the deposition frequency of the employed $V(t, \mathbf{s})$ hills will determine the accuracy of the free energy calculation.[7cd] In a sufficiently fine exploration the CV-s will automatically determine the lowest energy path from one energy basin to the next. Such simulations typically employ much smaller hill height than the lowest barrier on the explored hypersurface in the CV space. The accuracy can also be checked a posteriori. In this way the sequence of the elementary steps, together with the corresponding intermediates and transition states, is obtained within one simulation. We note that a coarse simulation (where the exploration of the underlying free energy surface is done with larger and wider $V(t, \mathbf{s})$ terms (see eq 1) does not necessarily lead to the lowest energy reaction path; however, the predicted paths from such a simulation can provide further ideas concerning alternative routes. In fact, in this study we also exploit this feature of the method.

The reaction mechanism as determined from experiment and ab initio calculation[5] is presented in Figure 2. In the first step of this scheme, the epoxide is activated by a Lewis acid and opened by the backside nucleophilic attack of the cobaltate anion. In the second and third steps carbonylation occurs and the coordination sphere of the cobaltate is resaturated with CO. In the fourth and final step the lactone is formed. In the present case we employed four independent CV-s, which are able to capture all the bond breakings and formations that link the reactants and the products. The coordinates were s_1, the CN of the Co atom relative to the epoxy carbon atoms; s_2, the CN between the epoxy carbons and the ligand carbon atoms; s_3, the CN of the epoxy oxygen and the ligand carbon atoms; and finally s_4, the CN of the Co with the gas-phase CO carbons. (For the definition of CN-s see the previous section.)

We performed a number of metadynamics simulations. The higher and larger Gaussians were used to perform fast exploratory searches. Then the free energy surface was refined using finer Gaussians, which lead to more expensive calculations. The results showed that the selected set of variables (s_1−s_4) can be separated into two sets, (s_1, s_2) and (s_3, s_4), as the corresponding elementary reaction steps do not overlap, but always exhibit a sequential order. In this way we could explore two 2D spaces, which allows us to obtain a better accuracy/efficiency relation. In such subsequent simulations we first obtain reaction paths in terms of the s_1 and s_2, then continue the simulation employing the s_3 and s_4 variables.

In Figure 3 we display the complete energy profile of the entire reaction pathway. It is clear that the energy path $\mathbf{I_1}$-$\mathbf{TS_1}$-$\mathbf{I_2}$-$\mathbf{TS_2}$-$\mathbf{I_4}$-$\mathbf{I_5}$-$\mathbf{TS_5}$-$\mathbf{I_7}$ obtained from the simulation reproduces well the reaction pathway proposed in Figure 2. However, the simulations provide us with extra information. First of all, we obtain insight into the dynamic aspects of the reaction. To this end, we present Figure 4, where we display the evolution of the coordination sphere of the central Co atom in a typical simulation. Several important events are featured on the trajectory. We identify the positions along the trajectory by the time in which they occur during the metadynamics. It must be stressed however that these are not physical times, but only a measure of the computational effort. As the simulation starts, within 1 ps we can observe the epoxy coordination to the Co atom, accompanied by the epoxy-ring opening ($\mathbf{I_2}$). In Figure 4 the first peak indicates this step. As we mentioned above, we have never observed CO coordination preceding the epoxy−Co bond formation. We conclude that to reach the five-coordinated state the Co prefers the formation of a σ-bond with the epoxy carbon atom to the coordination of a fifth CO molecule, where the interaction would be mainly due to the interplay of a σ-repulsion and π-back-donation.[16] Very soon however the β-alkoxy species migrates to one of the CO ligands, as shown also in Figure 3 ($\mathbf{I_4}$). In other words, a CO insertion into the Co−C bond takes place, thus reducing the CN of Co back to 4. At around 1.8 ps a side-on coordination of the α- and β-carbon atoms of the acyl species formed in the previous step is observed and indicated by the second peak in Figure 4. This suggests the preference of Co for higher coordination. Indeed, after 3 ps, the Co center stabilizes with the uptake of a fourth CO ligand from the gas phase, leading to a five-coordinated Co ($\mathbf{I_5}$). For a short period around 6 ps the Co center becomes four-coordinated, but this state is only very short-lived. At about 7 ps we observe a CO exchange, where a gas-phase CO molecule substitutes an original ligand CO. The S_{E2} feature of the exchange is apparent from Figure 4. Subsequently, within 3 ps the lactone formation occurs and the product dissociates from the catalytic site ($\mathbf{I_7}$). The lactone formation and the dissociation take place in a concerted manner: apparently the ester bond formation weakens the Co−C_α bond so significantly, and the lactone ring represents such a bulky group, that the dissociation becomes the favored route. In this way the active site becomes $Co(CO)_4^-$ again; that is, the original catalytic species is recovered. We also observe that as the dissociation occurs and the lactone ring starts to stabilize, the Lewis acid also leaves, due to the strong ester bond formation, which in turn weakens the oxygen−Lewis acid bond.

(16) Bagus, P. S.; Nelin C. J.; Bauschlicher, C. W., Jr. *Phys. Rev. B* **1983**, *28*, 5423−5438.

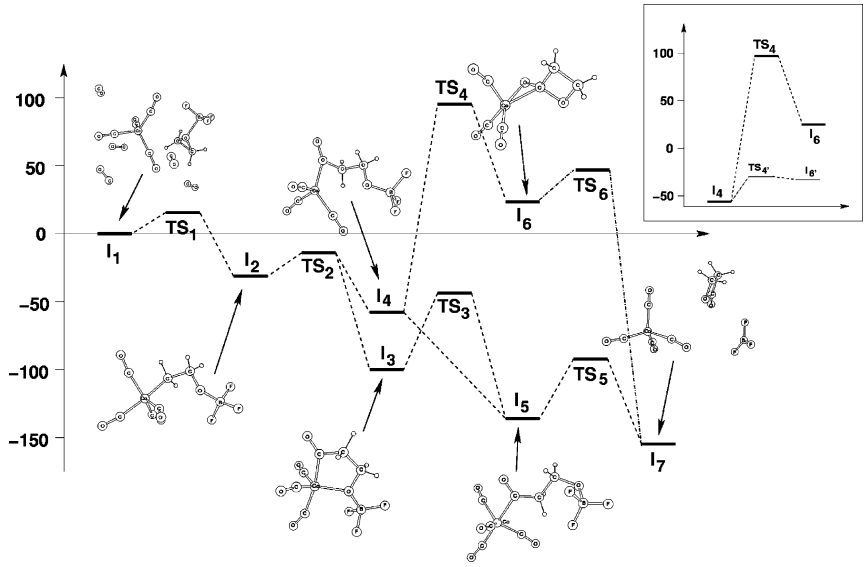

Figure 3. Complete energy profile for the reaction routes obtained from the metadynamics and from static simulations together with the optimized intermediate structures. Inset: Comparison of the barrier of the intramolecular lactone formation step in the presence of BF_3 and $B(CH_3)_3$. The reference energy level is chosen at $\mathbf{I_4}$, and the energy levels for $\mathbf{TS_{4'}}$ and $\mathbf{I_{6'}}$ (structures complexed with $B(CH_3)_3$ Lewis acid) are given relative to this level. In the case of $B(CH_3)_3$ we reoptimized the structure of the open intermediate ($\mathbf{I_4}$) with $B(CH_3)_3$.

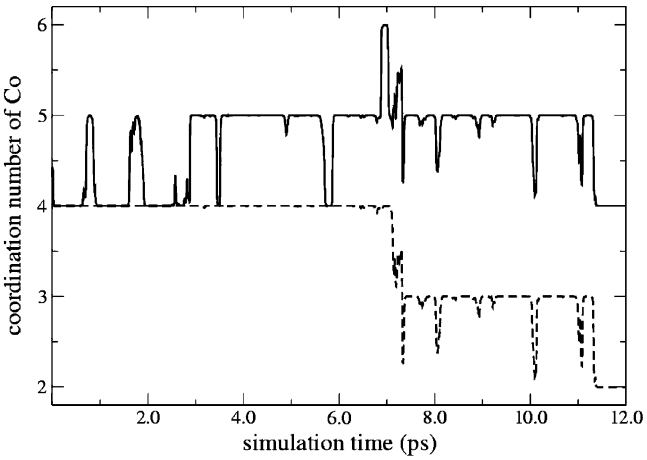

Figure 4. Evolution of the coordination sphere of the central cobalt atom in a simulation of 12 ps. The metadynamics parameters were the following: Gaussian hill height: 2.1 kJ/mol, perpendicular hill width: 0.08, Δt = 0.012 ps (simulation time before a new Gaussian is added). Solid line: CN of Co with respect to all carbon atoms; dashed line: CN of Co with respect to the carbon atoms of the initial carbonyl ligands. For definition of the coordination number see text. Here the reference Co−C distance R was set to 2.9 Å to obtain smooth profiles.

In parallel simulations we observed that the epoxy oxygen can perform an intramolecular attack on the central Co atom, forming a five-membered ring intermediate ($\mathbf{I_3}$) after the second step took place. This additional step has not previously been reported. We emphasize that the capture of this intermediate is owing to the nonzero temperature of the simulation, as the formation of $\mathbf{I_3}$ is independent of any change in the CV-s. Clearly, the intramolecular formation of the metalla-oxo-furanyl ring is facilitated by its greater stability with respect to the corresponding open chain intermediate ($\mathbf{I_4}$). The formation of this ring structure also reflects the Co preference for 5-fold coordination. Subsequently, the furanyl ring was opened by a CO uptake and the $\mathbf{I_5}$ open-chain isomer was obtained.

In a coarse simulation with lower sampling resolution we observed a different reaction mechanism for the third and fourth steps. This is a significant consequence of the fact that in a coarse simulation the reaction course does not necessarily follow the lowest energy path. In this trajectory the β-lactone ($\mathbf{I_6}$) remains on the cobalt site after its formation takes place. The Co center, which is four-coordinated when the ring formation occurs, is stabilized by an $\eta_{C,O}$ side-on coordination of the lactone ring. A subsequent electrophilic attack of a gas-phase CO molecule leads to the dissociation to the final products ($\mathbf{I_7}$) in a substitution reaction.

To reconstruct the energy profile of the reaction mechanism, stationary states were identified on the metadynamics trajectories by employing simple criteria: an apparent change in one or more of the collective coordinates (s_α), accompanied by the corresponding structural and energy changes. These configurations were then used as an input structure for further refinement with static quantum chemical methods. The most important energy values are summarized in Table 1, while the full energy profile is shown in Figure 3.

As we mentioned earlier, we have fully reproduced the reaction path obtained in our previous study ($\mathbf{I_1}$-$\mathbf{TS_1}$-$\mathbf{I_2}$-$\mathbf{TS_2}$-$\mathbf{I_4}$-$\mathbf{I_5}$-$\mathbf{TS_5}$-$\mathbf{I_7}$).[5] Now we focus on the additional reaction routes. The ($\mathbf{I_3}$) metalla-oxo-furanyl intermediate represents a 42 kJ/mol stabilization with respect to the ($\mathbf{I_4}$) open-chain form. This energy difference indicates that an equilibrium between $\mathbf{I_4}$ and $\mathbf{I_3}$ is strongly shifted toward $\mathbf{I_3}$. $\mathbf{I_3}$ transforms to $\mathbf{I_5}$ via a transition state of 55 kJ/mol. On the other hand, $\mathbf{I_4}$ can react with CO without any static energy barrier. This indicates a competition between the two possible directions for $\mathbf{I_4}$: intramolecular ring formation or intermolecular CO coordination. We also determined the energy profile of $\mathbf{I_4}$−$\mathbf{I_7}$ along the high-energy route. Along this pathway we observe the lactone formation taking place

Table 1. Summary of the Relative Energy Values along the Energy Profile Displayed in Figure 3[a]

	E (kJ/mol)		*E* (kJ/mol)
$\mathbf{I_1}$	0	$\mathbf{TS_1}$	14
$\mathbf{I_2}$	−38	$\mathbf{TS_2}$	−13
$\mathbf{I_3}$	−99	$\mathbf{TS_3}$	−44
$\mathbf{I_4}$	−57	$\mathbf{TS_4}$	+95
$\mathbf{I_5}$	−136	$\mathbf{TS_{4'}}$	−32
$\mathbf{I_6}$	+23	$\mathbf{TS_5}$	−92
$\mathbf{I_{6'}}$	−35	$\mathbf{TS_6}$	+45
$\mathbf{I_7}$	−154		

[a] The reference level is the energy level of the reactants ($\mathbf{I_1}$). Note that $\mathbf{TS_{4'}}$ is the activation barrier of the intramolecular lactone formation step when the alkoxy oxygen is complexed with $B(CH_3)_3$, calculated by reoptimizing the structures.

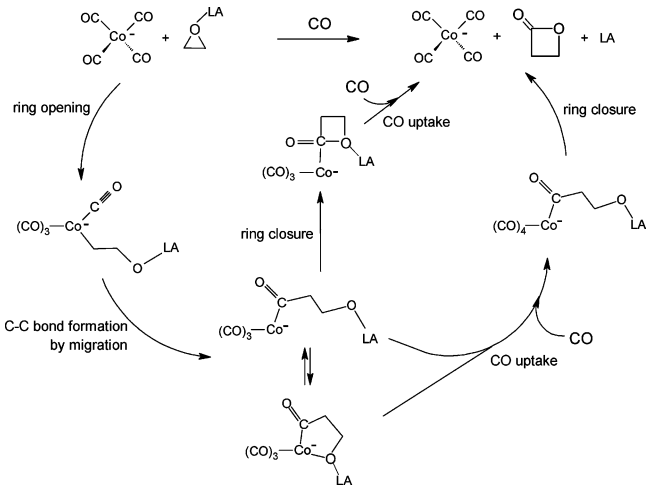

Figure 5. Amended reaction scheme.

through a transition state ($\mathbf{TS_4}$) where the Co center remains in a four-coordinated state. Note that in the static calculation another epoxide molecule has to be added to stabilize the leaving BF_3; otherwise the ring formation would not occur. The activation energy is relatively high (152 kJ/mol) and the reaction is endothermic ($\mathbf{I_6} - \mathbf{I_3} = +80$ kJ/mol). This result is in complete accord with the picture that emerged from the earlier calculations: the BF_3 molecule is among those Lewis acids that render the barrier for the lactone formation high. The strength of the Lewis acid essentially determines the barrier for the lactone formation, whereas the reaction on the Co site is not influenced directly by the Lewis acid. From previous results[5] we expect that other Lewis acids, such as $Al(^iPrO)_3$ or $B(CH_3)_3$, would yield much lower activation energy for this step. Indeed, if we recalculate the intramolecular lactone formation path starting from the open-chain form but complexed with $B(CH_3)_3$, we obtain 25 kJ/mol activation energy ($\mathbf{TS_{4'}}$) for the lactone formation, a value much smaller than that with BF_3 (Figure 3, inset). It is known[5] that the originally proposed $\mathbf{I_1}$-$\mathbf{TS_1}$-$\mathbf{I_2}$-$\mathbf{TS_2}$-$\mathbf{I_4}$-$\mathbf{I_5}$-$\mathbf{TS_5}$-$\mathbf{I_7}$ route features moderate (9−27 kJ/mol) activation energy and an overall high exothermicity in the presence of $B(CH_3)_3$. Consequently the calculated 25 kJ/mol barrier height relative to $\mathbf{I_4}$ (now complexed with $B(CH_3)_3$) indicates an effectively competitive route with this Lewis acid. This barrier is even smaller than the barrier for the $\mathbf{I_3}$-$\mathbf{TS_3}$-$\mathbf{I_5}$ transformation by 30 kJ/mol. Proceeding along this pathway, the next step is that the Co catalyst and the resulting lactone have to eventually dissociate. During the course of the dynamical simulations, dissociation was always induced by CO uptake. For this step we obtained a moderate 22 kJ/mol activation energy and huge exothermicity, reflecting the high-energy nature of the route with the actual BF_3 Lewis acid. In short, the lactone formation and the CO uptake may occur in reverse order compared with the reaction mechanism shown in Figure 2. As the comparison of the BF_3 and $B(CH_3)_3$ shows, the softer $B(CH_3)_3$ Lewis acid renders the lactone formation much easier than the same process with the hard BF_3, opening in this way a competing route between states $\mathbf{I_4}$ and $\mathbf{I_7}$. This alternative route and the path featuring the metallafuranyl ring are now included in the original reaction pathway, thus providing a more complex picture for the reaction mechanism. The resulting reaction scheme is displayed in Figure 5.

Conclusions and Outlook

A novel ab initio metadynamics method has been applied to investigate the reaction mechanism of a homogeneous multisite catalytic process, the formation of β-lactone from epoxide. Due to the fairly unbiased nature of the approach, the simulations were able to provide not only the elementary steps of this multistep reaction but their temporal sequence as well. The calculations revealed that the lowest energy pathway found in ref 5 features an additional intermediate, namely, the product of an intramolecular ring closure, which represents a more favorable energetic state for the CO insertion product. The reaction proceeds through a barrier of 55 kJ/mol from this intermediate toward the $\mathbf{I_5}$ state as opposed to the other possible, but barrierless $\mathbf{I_4}-\mathbf{I_5}$ step. With coarse simulations we have discovered another route, where the intramolecular lactone formation precedes the CO attack on the Co site. We verified that the competitiveness of this route strongly depends on the hardness of the Lewis acid, as the reactivity of the lactone oxygen is strongly influenced by the strength of its bond with the Lewis acid.

We emphasize that such simulations provide a very intuitive way to follow the course of the reactions by watching the trajectories and observing the reaction mechanism unravel. For instance, the importance of certain dynamical effects, such as the rotation of the carbon chain forming the lactone ring, is immediately grasped by visual inspection. The degree of prejudice incurred by chemical intuition is greatly reduced by selecting very general reaction coordinates that operate simultaneously, and thus more complete reaction pathways can be observed. Finally we note that the present approach to speed up the occurrence of rare events, which is equivalent to a sampling of the most important parts of the energy hypersurface, is general and can be applied in principle to arbitrary chemical reactions.[17]

Supporting Information Available: The complete trajectory of the reaction sequence and the coordinates for the stationary points are collected in the Supporting Information. This material is available free of charge via the Internet at http://pubs.acs.org.

OM0502234

(17) Stirling, A.; Iannuzzi M.; Laio A.; Parrinello M. *ChemPhysChem* **2004**, *5*, 1558−1568. Churakov, S.; Iannuzzi M.; Parrinello M. *J. Phys. Chem. B* **2004**, *108*, 11567−11574. Boero, M.; Ikeshoji T.; Liew C. C.; Terakura K.; Parrinello M. *J. Am. Chem. Soc*. **2004**, *126*, 6280.